Electronic Supplementary Material (ESI) for Journal of Materials Chemistry A.

Supporting Information

Unique Hollow Ni-Fe@MoS$_2$ Nanocubes with Boosted Electrocatalytic Activity for N$_2$ Reduction to NH$_3$

Libin Zeng[†, ‡], Xinyong Li[†, ‡], Shuai Chen[†], Jiali Wen[†], Wei Huang[†] and Aicheng Chen[*†]

[†] Electrochemical Technology Center, Department of Chemistry, University of Guelph, 50 Stone Road East, Guelph, ON N1G 2W1, Canada

[‡] State Key Laboratory of Fine Chemicals, Key Laboratory of Industrial Ecology and Environmental Engineering (MOE), School of Environmental Science and Technology, Dalian University of Technology, Dalian 116024, China

* Corresponding Author. aicheng@uoguelph.ca (A. Chen)

Experimental Section

Chemicals

Nickel nitrate hexahydrate ($Ni(NO_3)_2 \cdot 6H_2O$), sodium citrate (CH_3COONa), potassium hexacyanoferrate (III) ($K_4Fe(CN)_6$), N,N-dimethylformamide (DMF), sodium sulfate (Na_2SO_4), sodium hydroxide (NaOH), sodium salicylate ($C_7H_5O_3Na$), sodium hypochlorite (NaClO), sodium nitroferricyanide (III) ($C_5FeN_6Na_2O$) and ammonium chloride (NH_4Cl) were purchased from Sigma-Aldrich Chemical Reagent Co., Ltd. Nafion (1 wt.%) solution, hydrogen peroxide (H_2O_2), sulfuric acid (99.99%) and ethanol were purchased from Aladdin Ltd. Ammonium tetrathiomolybdate ($(NH_4)_2MoS_4$) was purchased from New Jersey (USA). All reagents were of analytical grade and used without further purification. Additionally, a cation exchange membrane (CEM) was purchased from the DuPont Company. Deionized water (18.2 MΩ cm) was used in the preparation of all the solutions.

Electrochemical measurements

The electrochemical characterization and activity test of as-prepared Ni-Fe-MoS_2 samples were carried out in a three-electrode cell (100 mL) by the electrochemical workstation (Voltalab Potentiostat PGZ301) with the required gas inflow system. To prepare the working electrode, the synthesized catalysts were coated on a glassy carbon electrode (3 mm). 5 mg as-prepared sample was dispersed in a mixed 480 μL water, 480 μL ethanol and 40 μL Nafion solution under continuous sonication for 40 min, then 10 μL obtained catalytic ink was drop-coated onto the glassy carbon electrode surface, and finally dried at room temperature. A Ag/AgCl (1 M KCl) and graphite rod (3 mm) were employed as the reference and counter electrodes, respectively. The applied electrolysis potential was converted to the reversible hydrogen electrode (RHE), $E_{RHE} = E_{Ag/AgCl} + (0.222 +$

0.059*pH) V. A 0.1 M Na_2SO_4 solution was selected as the electrolyte for all electrochemical experiments. For the nitrogen reduction reaction (NRR) measurements, highly pure nitrogen gas (99.999%) was purged into the electrolyte solution for 30 min prior to each electrochemical experiment. As the NRR and the hydrogen evolution reaction (HER) occur simultaneously, to estimate the dgree of the HER, the same electrochemical measurements were carried out in an argon-saturated solution. Linear sweep voltammetry (LSV) was employed to evaluate the catalytic activity under Ar- and N_2-saturated conditions (sweep rate: 10 mV s^{-1}). In addition, electrochemical impedance spectroscopy (EIS) was used to analyze the electron transfer resistance during the NRR (10^{-2} - 10^5 Hz).

Characterization of nanomaterials

A field-emission scanning electron microscope (FE-SEM) (Nova Nano SEM450, USA) equipped with energy dispersive X-ray spectroscopy (EDS) and the high-resolution transmission electron microscopy (HRTEM) (FEI Tecnai F30 electron microscope, using a 200 kV accelerating voltage) were employed to characterize the morphology, composition and structure of the as-prepared Ni-Fe@MoS_2 NCs catalysts. X-ray diffraction (XRD) with a diffractometer with Cu $K\alpha$ radiation (D/max-2400, Japan, source light at the wavelength (λ) of 0.1541 nm) was used to analyze the crystalline structure. The chemical composition and oxidation states of the as-prepared Ni-Fe@MoS_2 NCs were further investigated by X-ray Photoelectron Spectroscopy (XPS) (Thermo ESCALAB 250XI, USA). The specific surface area and pore size distribution were elucidated by nitrogen adsorption/desorption isotherms using a Quantachrome instrument (NOVA 4200e, USA). Raman spectra were recorded at 532 nm by utilizing an inVia Raman spectrophotometer (Renishaw Canada

Ltd.). The photoluminescence spectra (PL) were probed by the photoluminescence spectrophotometer (Hitachi FL-4500, excited at λ = 360 nm) at room temperature.

Electrochemical activity evaluation

For the NRR test, an H-type two chamber device separated by a pre-treatment CEM was employed to investigate the products.[1] The generation of ammonia (NH_3) product in the cathode chamber was measured and quantitatively analyzed via the indophenol blue method.[2, 3] As following, 2.0 mL of cathode effluent was added to 2.0 mL of 10.0 g salicylic acid and 10.0 g sodium citrate dissolved in 0.32 M NaOH solution. Next, 1.0 mL of 0.05 M NaClO and 0.2 mL of 0.01 g mL^{-1} $C_5FeN_6Na_2O$ were introduced dropwise into the testing solution in turn. After two hours, the mixture was measured at 655 nm using a UV-vis spectrophotometer. Further, a series of standard NH_4Cl concentration (0.0 - 1.0 μg mL^{-1}) vs. UV-vis absorbance peak were performed by a well-fitting linear relation curve ($y = 0.113\ x + 0.013$, $R^2 = 0.999$) in parallel triplicate experiments to determine the concentration of NH_3 generation ($C^{[NH_3^{N2}]}$). To elimate the possible endogenous sources interference,[4] the corresponding Ar-condition ($C^{[NH_3^{Ar}]}$) and the open circuit condition of N_2-saturated condition ($C^{[NH_3^{Open}]}$) for the NRR experiment were used as the baseline for NH_3 yield determination. The exact $C[NH_3]$ generated by the NRR was calculated using Equation 1:

$$C[NH_3] = C^{[NH_3^{N2}]} - C^{[NH_3^{Ar}]} - C^{[NH_3^{Open}]} \qquad [1]$$

The NH_3 yield was calculated by Equation 2:

$$NH_3\ \text{yield} = C_{[NH_4^+]} \times V / (m_{cat.} \times t) \qquad [2]$$

where $C_{[NH_4^+]}$ is the calculated NH_3 concentration; V is the reaction electrolyte solution; $m_{cat.}$ is the loading catalyst content, and t is the electrolysis reaction time.

Faraday efficiency was obtained by Equation 3:

$$\mathrm{FE} = 3\times\mathrm{F}\times C_{[NH_4^+]} \times \mathrm{V}/\,(18 \times \mathrm{Q}) \qquad [3]$$

where F refers to the Faraday constant (96485.3 C mol^{-1}); Q is the quantity of electric charge via the applied potential. Meanwhile, triplicate experiments were performed to evaluate the generation of NH_3 yields.

Additionally, the possible by-product (N_2H_4) was investigated by our previously reported method.[1] At 455 nm, there are no changes or new signal generation for the initial and two-hour for the NRR in the UV-vis spectrum, which suggested that negligible N_2H_4 was generated in the NRR over Ni-Fe@MoS_2 NCs.

Table S1. Physical properties of the Ni-Fe PBA and Ni-Fe@MoS_2 samples.

Sample	**Surface areas (m^2 g^{-1})**	**Pore volume (cm^3 g^{-1})**	**Pore radius (nm)**
MoS_2	6.26	0.07	3.27
Ni-Fe PBA-Air	32.37	0.14	5.11
Ni-Fe PBA-Ar	33.87	0.03	5.18
Ni-Fe-MoS_2 NCs	31.51	0.14	4.54

Table S2. Analysis of the deconvoluted elemental peaks from XPS and their relative atomic percentage in terms of Ni-Fe PBA and Ni-Fe@MoS$_2$ NCs (before and after the NRR) catalysts.

Samples	**Ni-Fe PBA**	**Ni-Fe@MoS$_2$ (Before)**	**Ni-Fe@MoS$_2$ (After)**
C (%)	48.42	39.95	41.02
N (%)	35.58	28.60	28.54
Fe (%)	8.82	8.24	8.21
Ni (%)	7.18	6.14	6.03
Mo (%)	-	5.03	5.01
S (%)	-	12.04	11.19

Table S3. Calculated adsorption energy of the $Ni_{\alpha}Fe_{1-\alpha}$-MoS_2 samples.

$Ni_{\alpha}Fe_{1-\alpha}$-MoS_2	Adsorption energy (eV)
$\alpha=0.5$	532.65
$\alpha=0.4$	217.56
$\alpha=0.3$	-102.13
$\alpha=0.2$	-574.02
$\alpha=0$	-1069.4

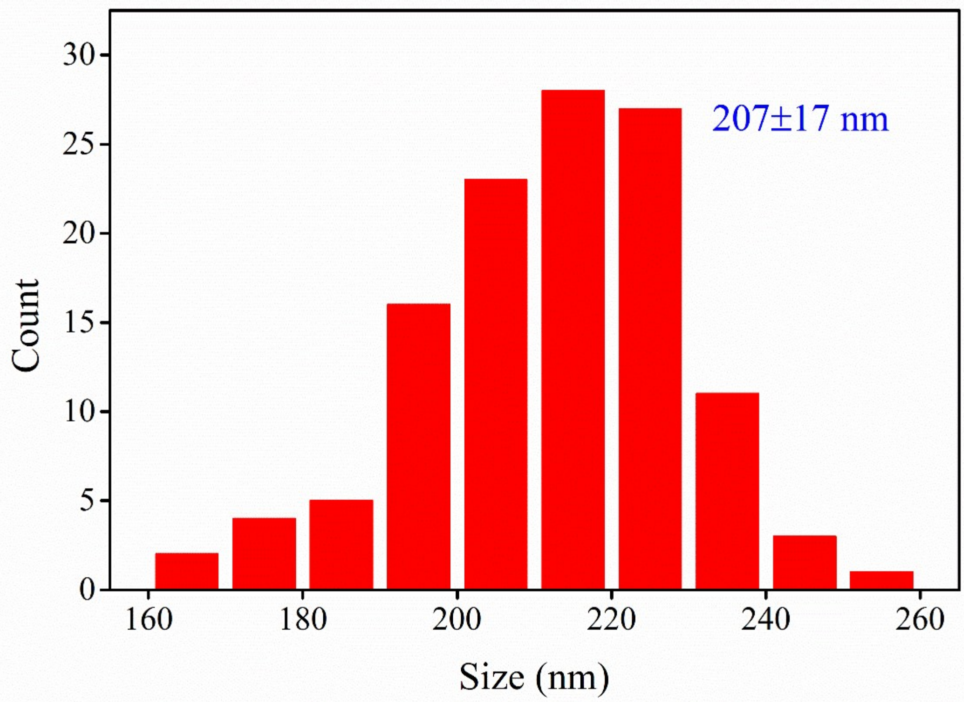

Figure S1. Size distributions of as-prepared NiFe-PBA templates.

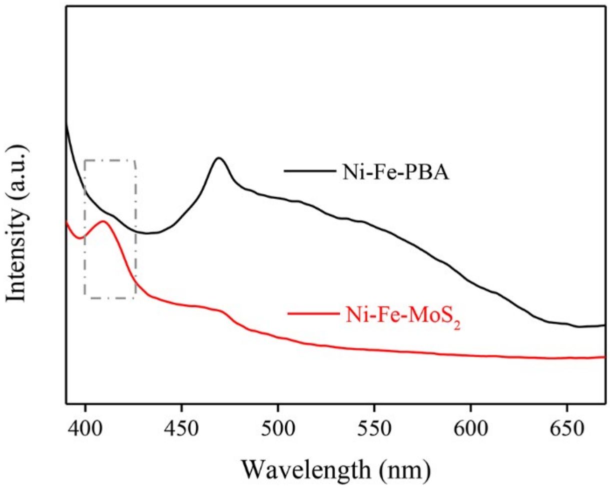

Figure S2. Photoluminescence spectra of the as-prepared Ni-Fe-PBA and Ni-Fe-MoS$_2$ samples recorded at an excitation wavelength of 360 nm.

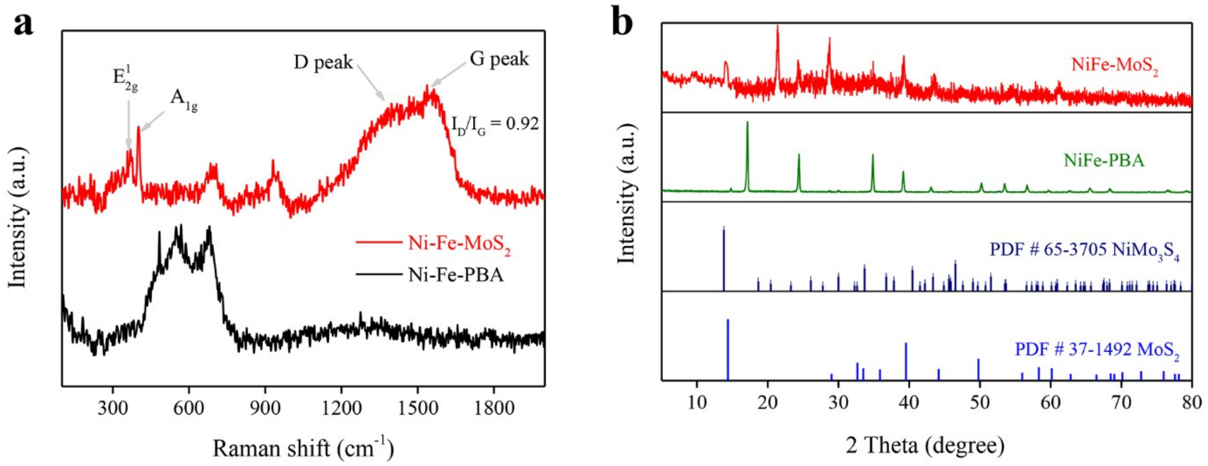

Figure S3. (a) Raman spectra of Ni-Fe-MoS$_2$ NCs and Ni-Fe-PBA samples excited at 532 nm; (b) the corresponding XRD patterns.

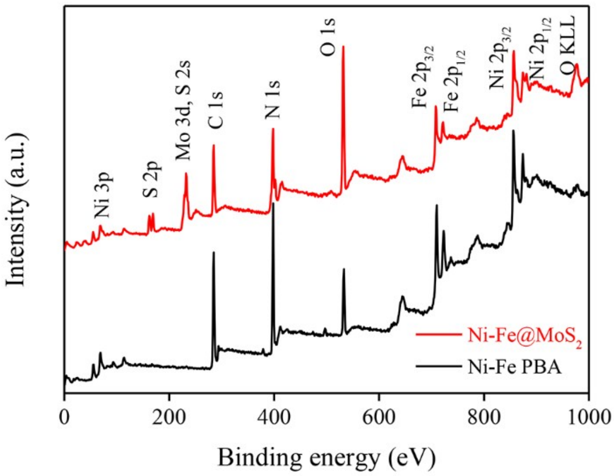

Figure S4. XPS survey of the as-prepared Ni-Fe-PBA and Ni-Fe-MoS$_2$ catalysts.

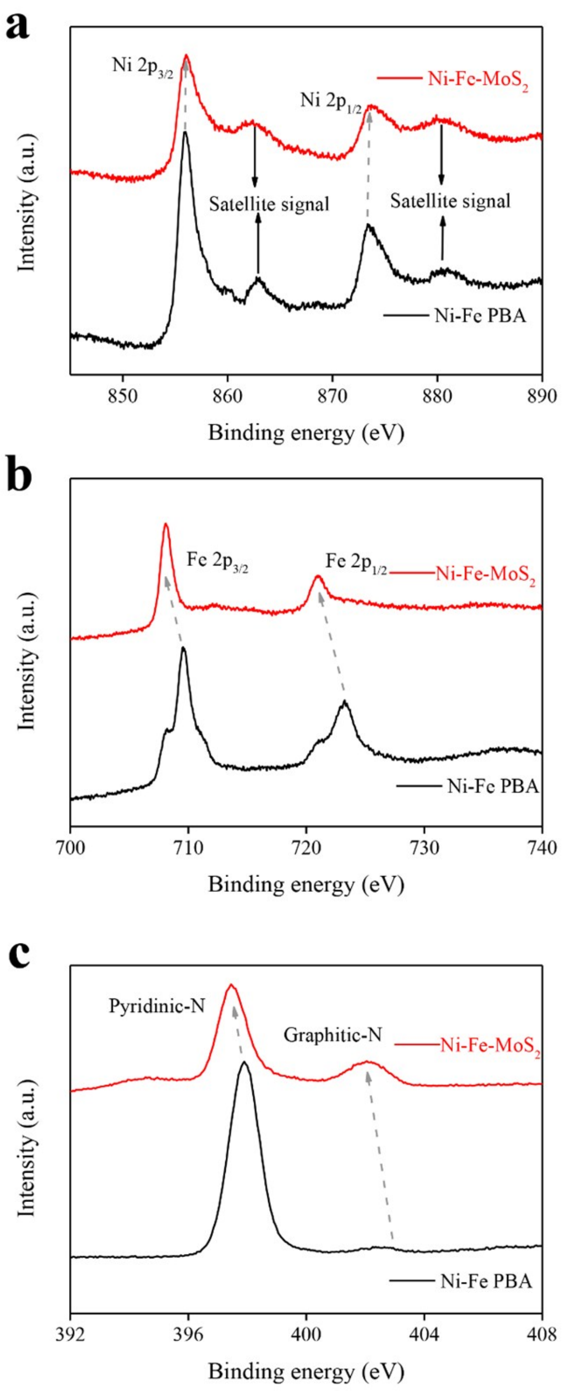

Figure S5. High-resolution XPS spectra and the fitted spectra of N 1s (a), Ni 2p (b) and Fe 2p (c) for the Ni-Fe PBA and Ni-Fe-MoS_2 samples, respectively.

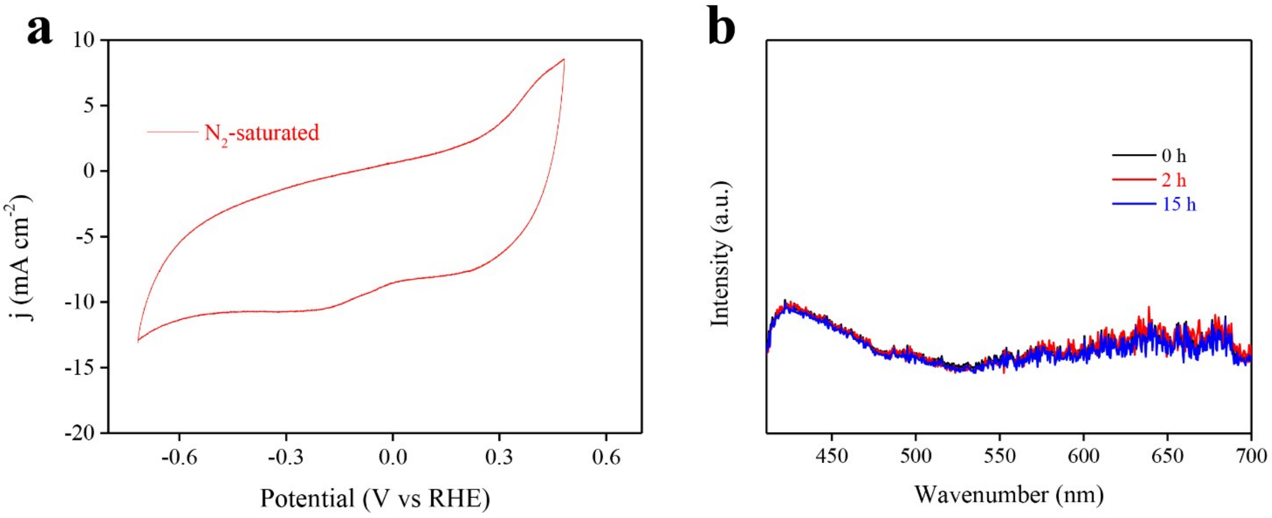

Figure S6. (a) Cyclic voltammogram of NiFe-MoS$_2$ NCs under N$_2$-saturated condition; (b) UV-vis absorption spectra of the electrolytes estimated by the N$_2$H$_4$ generation, prior to and following the NRR under N$_2$ atmosphere at -0.3 V vs RHE with 0.1 M Na$_2$SO$_4$ solution as the background.

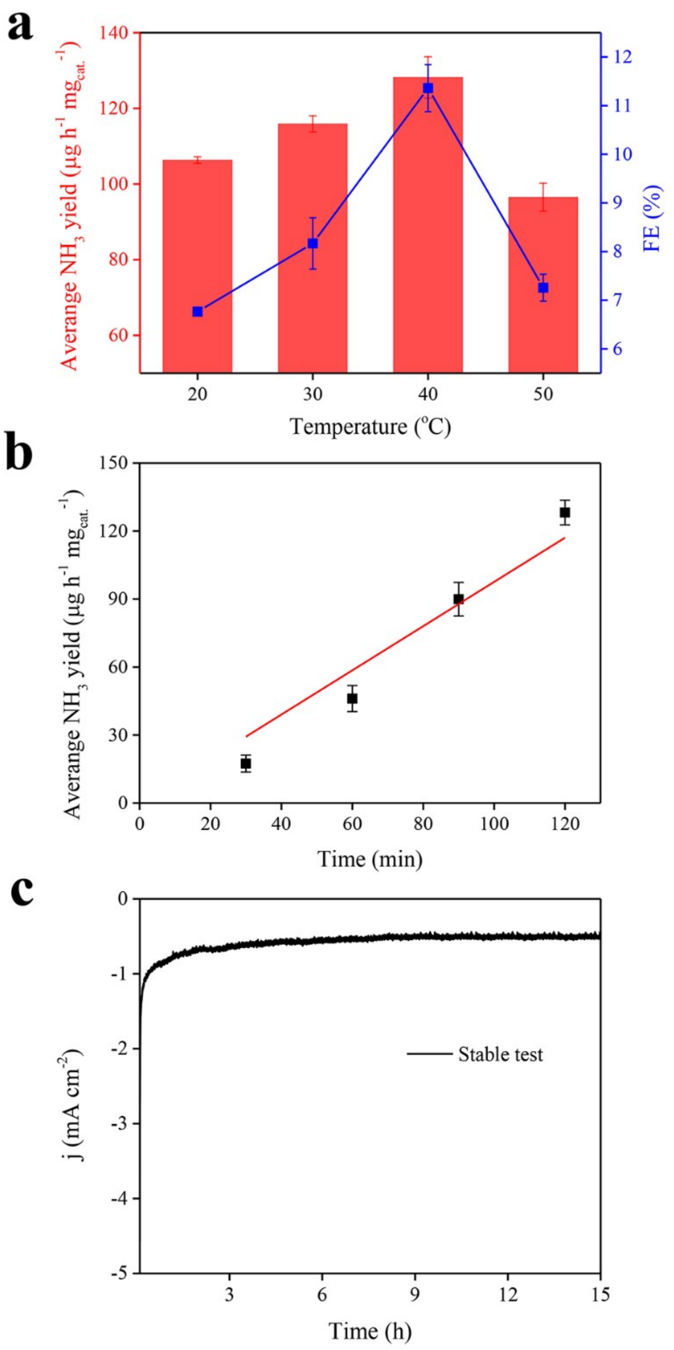

Figure S7. (a) NH_3 yields and corresponding FEs of the Ni-Fe-MoS_2 NCs in 2 h at -0.3 V vs RHE under different electrolysis temperature; (b) the amount of NH_3 versus reaction time at -0.3 V at at 40 °C condition; (c) current density dependent time curve of the NiFe@MoS_2 catalyst during 15 h at -0.3 V vs. RHE. Error bars refer to the standard deviation among the three replicates.

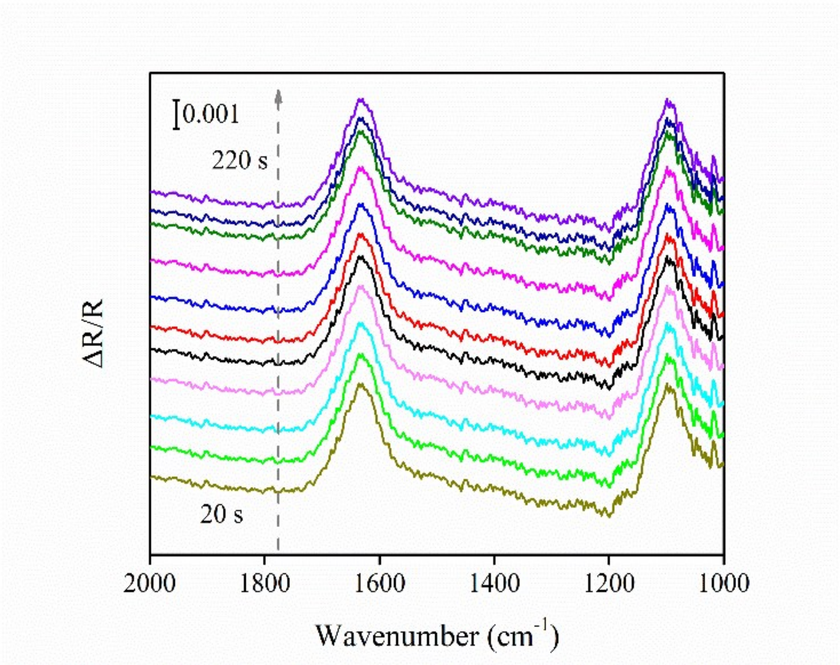

Figure S8. *In situ* electrochemical-FTIR spectra of the NRR on the Ni-Fe-MoS_2 NCs catalyst under Ar-saturated condition at -0.3 V.

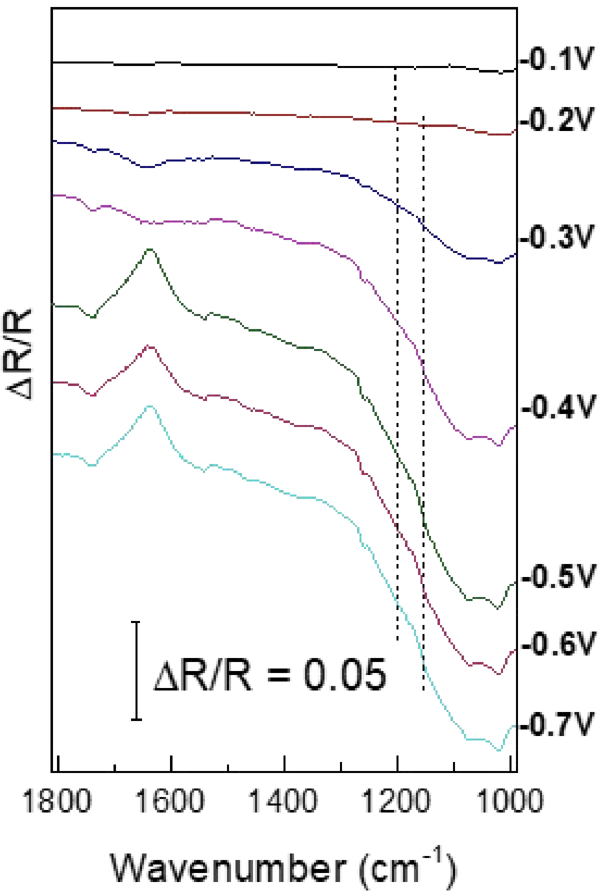

Figure S9. *In situ* electrochemical-FTIR spectra of the NRR on the Ni-Fe-MoS_2 NCs catalyst under different potentials with N_2-saturated conditions.

References

1. Zeng, L.; Chen, S.; van der Zalm, J.; Li, X.; Chen, A., *Chem. Commun.* 2019**, *55***, 7386-7389.

2. Wang, Z.; Li, Y.; Yu, H.; Xu, Y.; Xue, H.; Li, X.; Wang, H.; Wang, L., *ChemSusChem* 2018, ***11***, 3480-3485.

3. Xia, L.; Wu, X.; Wang, Y.; Niu, Z.; Liu, Q.; Li, T.; Shi, X.; Asiri, A. M.; Sun, X., *Small Methods* 2018, ***14***, 1800251.

4. Andersen, S. Z.; Colic, V.; Yang, S.; Schwalbe, J. A.; Nielander, A. C.; McEnaney, J. M.; Enemark-Rasmussen, K.; Baker, J. G.; Singh, A. R.; Rohr, B. A.; Statt, M. J.; Blair, S. J.; Mezzavilla, S.; Kibsgaard, J.; Vesborg, P. C. K.; Cargnello, M.; Bent, S. F.; Jaramillo, T. F.; Stephens, I. E. L.; Norskov, J. K.; Chorkendorff, I., *Nature* 2019, ***570***, 504-508.